

Revista UIS ingenierías

ISSN: 1657-4583 ISSN: 2145-8456

Universidad Industrial de Santander

Rezende-Lopes, Fernanda; Tannous, Katia; Rezende-Lopes, Thiago
Heat flow and specific heat capacity in the dehydration
stage of biomasses pyrolysis through thermal analyses
Revista UIS ingenierías, vol. 22, no. 1, 2023, January-March, pp. 57-68
Universidad Industrial de Santander

DOI: https://doi.org/10.18273/revuin.v22n1-2023006

Available in: https://www.redalyc.org/articulo.oa?id=553775346006



Complete issue

More information about this article

Journal's webpage in redalyc.org



Scientific Information System Redalyc

Network of Scientific Journals from Latin America and the Caribbean, Spain and Portugal

Project academic non-profit, developed under the open access initiative



Revista UIS Ingenierías



Página de la revista: https://revistas.uis.edu.co/index.php/revistauisingenierias

Heat flow and specific heat capacity in the dehydration stage of biomasses pyrolysis through thermal analyses Flujo de calor y capacidades calorífica específica en la etapa de deshidratación de la pirólisis de biomasas por análisis térmicos

Fernanda Rezende-Lopes ^{1a}, Katia Tannous ^{1b}, Thiago Rezende-Lopes ^{1c}

Laboratório de Tecnología de Partículas e Processos Multifásicos, Faculdade de Engenharia Química, Universidade Estadual de Campinas, Brasil. Orcid: 0000-0002-6867-3426 a, 0000-0003-0867-3261 b. Emails: f070842@dac.unicamp.br a, katia@feq.unicamp.br b, t157400@dac.unicamp.br c

Received: 2 July 2022. Accepted: 27 September 2022. Final version: 3 January 2023.

Abstract

This study aims to investigate the influence of the moisture of energy cane and coconut fiber on heat flow and specific heat capacity in the dehydration stage from the pyrolysis process. The experiments were carried out in a simultaneous thermogravimetry and differential scanning calorimetry analyzer using a heating rate of 20 K/min in an inert atmosphere. Three decomposition stages were identified: dehydration (marked by an expressive endothermic peak), pyrolysis, and carbonization. From the analyses of the water contributions, it was observed that the heat flow from the heat capacity of remaining water (Q_{wc}) is negligible compared to the heat flow from the water evaporation (Q_{we}) , for both biomasses. Also, we calculated the heat flow from the heat capacity (Q_b) and the experimental specific heat capacity (c_{p,b}) of biomasses such as 686-2371 J/kg K and 1076-2113 J/kg K, respectively. Then, for the dehydration stage, third- and fourth-order theoretical polynomial equations have been proposed to predict the heat required for the biomass heating.

Keywords: biomass; calorimetry; evaporation; heating; thermogravimetry.

Resumen

Este estudio tiene como objetivo investigar la influencia de la humedad de la caña energética y la fibra de coco sobre el flujo de calor y la capacidad calorífica específica en la etapa de deshidratación del proceso de pirólisis. Los experimentos se llevaron a cabo en un analizador simultáneo de termogravimetría y calorimetría diferencial de barrido utilizando una velocidad de calentamiento de 20 K/min en atmósfera inerte. Se identificaron tres etapas de descomposición: deshidratación (marcada por un pico endotérmico expresivo), pirólisis y carbonización. De los análisis de los aportes de agua se observó que el flujo de calor proveniente de la capacidad calorífica del agua remanente (Q_{wc}) es despreciable en comparación con el flujo de calor proveniente de la evaporación del agua (Q_{we}) , para ambas biomasas. Además, calculamos el flujo de calor a partir de la capacidad calorífica (Q_b) y la capacidad calorífica específica experimental $(c_{p,b})$ de las biomasas de 686-2371 J/kg K y 1076-2113 J/kg K, respectivamente. Así, para la etapa de deshidratación, se han propuesto ecuaciones polinómicas teóricas de tercer y cuarto orden para predecir el calor requerido para el calentamiento de las biomasas.

ISSN Printed: 1657 - 4583, ISSN Online: 2145 - 8456.



Palabras clave: biomasa; calorimetría; evaporación; calefacción; termogravimetría.

1. Introduction

Due to the growing demand for renewable energy sources, biomasses have stood out for being the only ones able to generate fuels, heat, and electricity [1]. The main thermochemical conversions for biomass include pyrolysis, combustión and gasification processes, respectively [2], [3]. In pyrolysis, the biomass is heated in an inert atmosphere and can generate following products: liquid (bio-oil), solid (biochar), and noncondensable gases [1], [4], [5].

In Brazil, biomass corresponds to approximately 30% of the energy matrix, mainly from sugarcane (19.1%) and firewood (8.9%). However, other biomasses such as rice husk and elephant grass represent only 3.0% of this matrix [6]. Among sugarcane species, energy cane (e.g., *Saccharum spontaneum* and *Saccharum robustum*) has a high fiber content (20-40 mass%) and low sucrose concentration (3-7 mass%), being more suitable for thermochemical processes and they are not useful for sugar production in traditional industries [7], [8]. Besides, energy cane has an advantage, it is easier farming without seasonality and rapid growth, and present high energy density and conversion efficiency [9].

Other biomass prosperous to integrate the Brazilian energy matrix is coconut shell residue since the production of the fruit was 2.5 million tons per year between 2010 and 2020 [10]. Approximately 85% of the fruit is disposed of in landfills. From the discarded material (epicarp, mesocarp, and endocarp), it is possible to take advantage of the fruit mesocarp (fiber) in thermochemical processes to produce biofuels and electricity. Their use mitigates the large volumes occupied in landfills and environmental problems (e.g., methane generation) related to their disposal [11].

Biomass in the natural state usually contain a considerable amount of moisture, and its content is an important factor in these processes, possibly affecting the performance and operational reliability of reactors [12]. Furthermore, the moisture content may influence the storage and transport of the material as well as the properties of bio-oil, reducing the heating value, making ignition difficult, and decreasing the liquid stability [13].

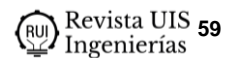
Besides that, according to Tabakaev et al. [14], the heat required for the heating and evaporation of moisture can represent from 19% to 32% of the total heat of pyrolysis. The dehydration is predominantly endothermic and demanding heat supply from external sources. Thus, it is

important to know the energy requirements at this process. In the literature, in general studies concerning the dehydration stage discuss its kinetics and propose biomass drying models [12], [15], [16], [17], [18]. However, few of them investigate the heat flow and specific heat capacity at this stage [15], [19], [20].

Artiaga et al. [19] and Cai and Liu [20] highlighted the stage, showing that, dehydration from thermogravimetry (TG) and differential scanning calorimetry (DSC) curves, it is possible to determine the heat flow from the water contributions (Q_w) , which is divided into two parts: one corresponding to the water evaporation (Q_{we}) and the other to the heat capacity of remaining water (Q_{wc}) . These authors evaluated these contributions in black fir forest residue and corn stalk/wheat straw, respectively. In this process stage (T<473 K), they observed that above 378 K, the heat flow from the water evaporation (Q_{we}) corresponded to about 100% of the heat flow obtained by DSC.

Besides that, the specific heat capacity (c_p) is a thermodynamic property that can be influenced by the biomass moisture; however, few studies have considered the water contributions in this property. Comesaña et al. [21] studied eight different biomasses (hazelnut shell, almond shell, olive stone, pinion, and pellet of oak poplar, pine, and brassica) and the three main lignocellulosic components (hemicellulose, cellulose, and lignin). The experiments were carried out using a TG-DSC (model Setaram Labsys, England) for a heating of 30K/min (from room temperature to 423 K) and simples of 20 mg. To determine the specific heat capacity, the authors considered that the heat flow obtained by this equipment (Q_{DSC}) refers to the heat flow from the heat capacity of biomass (Q_b) and water (Q_{wc}) , and the heat flow from the water evaporation (Q_{we}) . From these analyses, the authors excluded the heat flow from the water contributions (Q_w) and determined specific heat capacity as a function of the temperature, $c_p(T)$, considering polynomial equations between first- and fifth-order. These equations can, therefore, be used as a reference for this property to investigate other biomasses.

Dupont et al. [2] calculated the specific heat capacity (c_p) for twenty-one biomasses, such as corn stover, olive pomace, rice husk, switchgrass, and wheat straw, previously dried at 383 K for 2 h. The analyses were carried out in a calorimeter (model Calvet C80), in which biomass simples (1-2 g) were submitted to a heating rate of 0.2 K/min from 298 to 383 K. The authors found property between 1300 and 2000 J/kg K in the temperature range validated between 313 to 353 K.



Few studies concerning the influence of moisture on heat flow of biomass pyrolysis [19], [20] and its thermodynamic properties [2], [21] have been found in the literature. We can observe that experimental procedures vary widely among them, such as the mass from 5 mg [20] to 2000 mg [2]) and heating rate from 0.2 K/min [2] to 30 K/min [20], [21], affecting the data interpretation and accuracy.

Thus, this study aims to investigate the effect of the heating and evaporation of moisture of energy cane (Saccharum spontaneum) and coconut fiber (Cocos nucifera) on heat flow in the dehydration stage of biomass pyrolysis. Firstly, the global assessment of the biomass decomposition profiles, and thermal events (endothermic and exothermic) were carried out through simultaneous thermogravimetry and differential scanning calorimetry (TG-DSC) analyzer. Recommendations of the ASTM were applied to guarantee greater precision of the results. Secondly, the heat flow from the heat capacity (Q_{wc}) and evaporation (Q_{we}) of water, and heat flow from the heat capacity of biomasses (Q_b) as a function of the temperature were determined. Finally, experimental specific heat capacity of biomasses $(c_{p,b})_{exp}$ were defined and from them, theoretical polynomial equations $(c_{p,b})_{theo}$ were proposed as a function of the temperature. The knowledge of these properties will help researchers in estimating the heat required for the biomass heating in the initial stage of pyrolysis as well as in the design of pyrolytic reactors.

2. Material and Methods

2.1. Material

The raw materials selected for this study were energy cane Saccharum spontaneum and coconut fiber, in which chemical and thermal properties (Table 1) were detailed by Guimarães and Tannous [9] and Lopes and Tannous [22], [23], respectively. Energy cane was planted in the Institute of Biology at University of Campinas, UNICAMP (22°49'03"S 47°04'11W), and the coconut husks were collected in the leisure areas of the Campinas city/SP (22°54'23"S, 47°3'42"W) and defibrated in the Food Packaging Laboratory in the School of Food Engineering (FEA/UNICAMP). Both materials were ground in knife mills of the Marconi (model MA 620, Brazil) and Rone (model NFA 1633, Brazil) brands, respectively, and then sieved (Granutest/Bertel, Brazil). From the screening, the samples retained between 0.30 and 0.21 mm (mesh -48+65) were selected. After that, the samples were dried in an oven (model Quimis Q314M-242, Brazil) at 376.0±1.0 K for 24 and 22 hours, respectively, until the final mass variation mass to reached less than 0.2% (ASTM E871-82 method).

Table 1. Ultimate and proximate analyses and heating values of energy cane and coconut fiber on a dry basis

Properties	Energy cane ¹	Coconut fiber ²		
Ultimate analysis (mass%)				
Carbon	43.5±0.2	46.5±0.2		
Hydrogen	6.3±0.0	6.9±0.3		
Nitrogen	0.1±0.0	0.4 ± 0.0		
Sulfur	-	0.2±0.1		
Ash	1.6±0.0	2.9±0.4		
Oxygen (by difference)	48.6±0.2	43.1±0.0		
Proximate analysis (mass%)				
Volatile matter	84.7±0.1	79.6±2.1		
Ash	1.6±0.0	2.9±0.4		
Fixed carbon	13.7±0.1	17.5±2.4		
Heating Value, HV (MJ/kg)				
Higher, HHV	17.3±0.7	17.7±0.1		
Lower, LHV	16.0±0.7	16.5±0.1		

¹Source: Guimarães and Tannous [9], with permission from Springer. ²Source: Lopes and Tannous [22], with permission from Elsevier.

2.2. TG-DSC analyses for biomass pyrolysis

The thermal decomposition analyses of energy cane and coconut fiber were performed on a TG-DSC equipment (Mettler Toledo, Switzerland, precision of ± 0.15 K and microbalance sensitivity ± 0.1 μ g), which has controlled temperature programming and records the mass variation and heat flow as a function of the temperature and time (intervals of 1s).

The samples of energy cane (29.5296 mg) and coconut fiber (10.0024 mg) were placed in a platinum crucible (70 µL) with a perforated lid and distributed to ensure a uniform distribution within this (2/3 of space). Different initial mass was applied for each biomass due to its distinct geometric shapes necessary to accommodate in crucible. The samples were submitted to 10 min isotherm at the initial and final temperatures of analyses and at a heating rate of 20 K/min. This heating rate was chosen according to ASTM E1269-11 (2018), which is more accurate. The temperatures applied were between room temperature (298 K) and final temperature (823 K). The experiments were performed in an inert atmosphere using nitrogen of 99.996% purity (4.6 FID), White Martins Gases Industriais Ltda (Praxair, Brazil) at a flow rate of 50 mL/min.

In addition, to calculate the specific heat capacity by ASTM E1269-11 (2018), it was also necessary to obtain the experimental curves of baselines, performing with empty crucible and synthetic sapphire discs 20.73±0.01

mg (Mettler Toledo, Switzerland) under the same conditions of biomasses. We highlight that the baselines were also established to avoid the buoyancy effects revealing an apparent mass gain in thermogravimetric analyses [24].

To verify the repeatability of the experiments, some analyses were carried out in duplicate showing consistency in the standard deviation of temperature $(\pm 0.77 \text{ K})$ and mass $(\pm 0.012 \text{ mg})$ at 298-823 K.

2.3. Data analysis

Firstly, the experimental data from the simultaneous thermogravimetry (TG) and the differential scanning calorimetry (DSC) of samples and sapphire were corrected by subtracting the experimental baselines. Secondly, these data were normalized according to equations (1), (2) and (3), respectively, in which m_0 is the mass at the initial temperature (T_0), and m, dm/dt, and q_{DSC} , the mass (mg), mass variation in relation to time t (mg/s), and experimental heat flow (mW) for different times t (s), respectively. The normalized mass was represented by W (-), the normalized mass loss rate by dW/dt (1/s), and the normalized heat flow by Q_{DSC} (mW/mg).

$$W = \frac{m}{m_0} \tag{1}$$

$$\frac{dW}{dt} = \frac{dm}{dt} \frac{1}{m_0} \tag{2}$$

$$Q_{\rm DSC} = \frac{q_{\rm DSC}}{m_0} \tag{3}$$

The experimental data processing for the determination of the heat flow and of the specific heat capacity were performed using the software Microsoft Excel Office 365 MSO (version 16.0.12130.20232).

2.4. Determination of heat flow from water contributions

In the first stage of pyrolysis (dehydration), the original sample can be divided into two types of components: one corresponding to water and the other to the solid sample.

The heat flow from heat capacity and water evaporation are responsible for a large part of the total heat flow. Therefore, this section shows the determination of the heat flow from water contributions (heat capacity and evaporation) of energy cane and coconut fiber.

To evaluate the water contributions in the dehydration stage of both biomasses, initially, it was identified by normalized mass loss rate, the point correspondent to the water-free (wf) biomasses dW/dt=0, as shown in Figures 1(a) and 1(c). After that, it was possible identify in the same figure the temperature T_{wf} (K) and the normalized mass W_{wf} (-), according to Artiaga [19].

The normalized heat flow from experimental data, Q_{DSC} (mW/mg), equation (4), was given by the sum of the heat flow from the heat capacity of biomass, Q_b (mW/mg), and heat flow from the water contributions, Q_w (mW/mg) [19], [21].

In turn, the latter parameter, equation (5), was determined by the sum of the heat flow from the heat capacity of remaining water, Q_{wc} (mW/mg), in which is the heat required to increase the temperature of the sample water, and the heat flow from the water evaporation, Q_{we} (mW/mg), correspondent to the heat required to change the phase of water present in the sample.

$$Q_{DSC} = Q_b + Q_w \tag{4}$$

$$Q_{w} = Q_{wc} + Q_{we}$$

$$= -\left(W_{w}c_{p,w}\frac{dT}{dt}\right)$$

$$+\left(H\frac{dW}{dt}\right)$$
(5)

$$W_w = W + W_{wf} \tag{6}$$

In these equations, W_b is the normalized mass (-) and $c_{p,b}$ is the specific heat capacity (J/kg K) of biomass. W_w is the normalized water mass (-), given by equation (6), $c_{p,w}$ is the water specific heat capacity (J/kg K); dT/dt is the heating rate (K/s), dW/dt is the normalized mass loss rate (1/s), H is the evaporation enthalpy (J/kg), and T is the temperature (K) at different times t (s).

Since the water specific heat capacity $(c_{p,w})$ variation is very small with the increase in temperature, we assumed in this study as a constant value of 4187 J/kg K, as reported in the literature [14], [19], [20]. For the enthalpy of water evaporation (H_w) , was adopted the equation (7), obtained through thermodynamic properties tables and diagram of water and steam for the temperature range between 289 and 443 K [20].

$$H_w (J/kg) = 3.18x10^{-3}T^2 - 320T + 2.82x10^6$$
 (7)

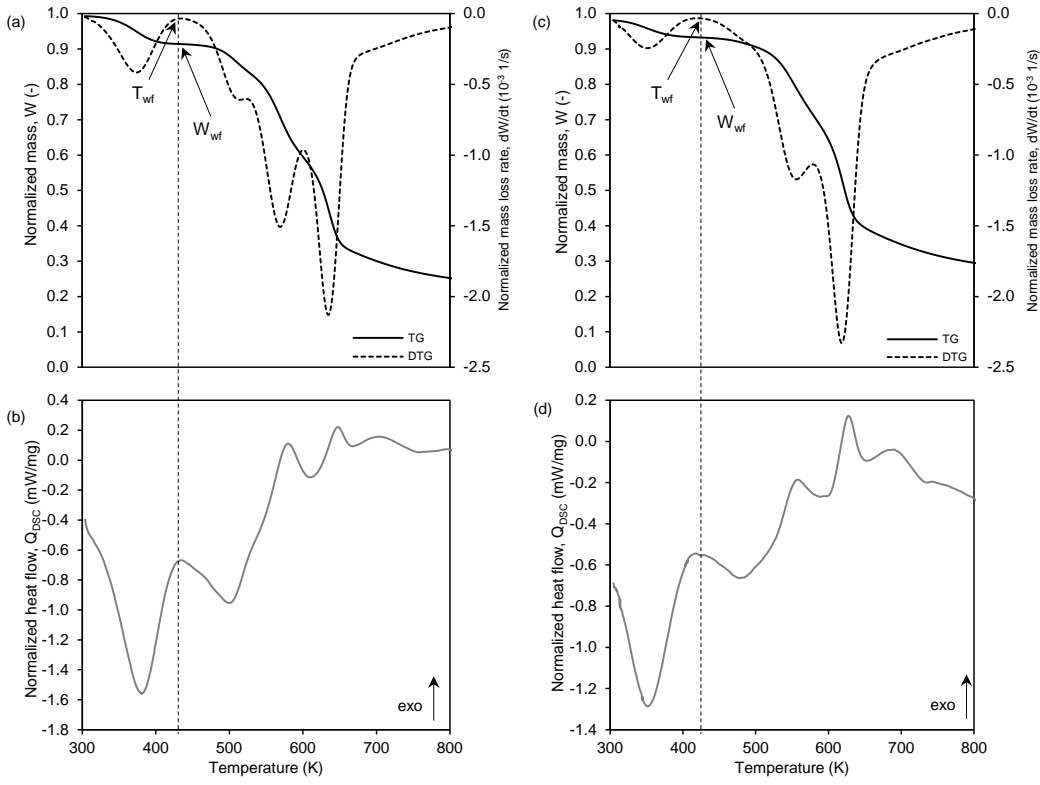


Figure 1. Normalized mass (W) and normalized mass loss rate, dW/dt, and normalized heat flow, Q_{DSC} , as a function of temperature of the thermal decomposition, energy cane (from Guimarães and Tannous [9], with permission of Springer) (a-b) and coconut fiber (from Lopes and Tannous [22] and Lopes and Tannous [23], with permission of Elsevier) (c-d).

2.5. Determination of specific heat capacity of biomasses $(c_{p,b})$

Firstly, to define the specific heat capacity $(c_{p,b})$ of biomasses in the dehydration stage was necessary to obtain the heat flow from the heat capacity of biomasses (Q_b) by subtracting of heat flow from the water contributions (Q_w) and the heat flow from the experimental data (Q_{DSC}) , according to equation (4) or $Q_b = Q_{DSC} - Q_w$.

After that, the $c_{p,b}$ was defined by two experimental approaches: (1) by classical definition, equation (8), that represents the amount of heat required for a unit of mass (1 g) of a given substance to increase its temperature by 1 K; (2) by standard ASTM E1269-11 (2018), equation (9), as recommended in the literature. In this equation, the variables are related to W_b and W_{ref} , the normalized masses (-), and Q_b and Q_{ref} , the normalized heat flow (mW/mg), and $c_{p,b}$ and $c_{p,ref}$, the specific heat capacity (J/kg K), of the biomasses and sapphire, respectively.

$$c_{p,b}(J/kg\,K) = -\frac{Q_b}{W_b\frac{dT}{dt}} \tag{8}$$

$$c_{p,b}(J/kgK) = \frac{W_{ref}}{W_b} \frac{Q_b}{Q_{ref}} c_{p,ref}$$
 (9)

The standard ASTM E1269-11 (2018) presents the sapphire specific heat capacity, $c_{p,ref}$, from 150 K to 1000 K, with intervals of 10 K. For obtaining new data with different temperature ranges, a fourth-degree polynomial curve (R^2 =1.0), equation (10), was established using least squares method of the software Microsoft Excel Office 365 (version 16.0.12130.20232).

$$c_{p,ref}(J/kg K) = -4.0x10^{-9} T^4 + 1.0x10^{-5} T^3 - 1.4x10^{-2} T^2 + 7.7 T - 566$$
 (10)

After determination of the experimental $c_{p,b}$, from equations (8) and (9), theoretical polynomial equations were proposed using least squares method definition of the software Microsoft Excel Office 365 MSO (version 16.0.12130.20232).

3. Results and discussion

3.1. Thermal decomposition analysis

Figures 1(a) and 1(c) show the normalized mass (W), mass loss rate (dW/dt), and Figures 1(b) and 1(d) show heat flow (Q_{DSC}) curves of energy cane and coconut fiber, respectively. Three main decomposition stages were observed for both biomasses, energy cane (304-821 K) and coconut fiber (305-824 K): dehydration, volatilization, and carbonization. More details concerning to the kinetics of thermal decomposition can be seen in Guimarães and Tannous [9] and Lopes and Tannous [22], respectively.

The first stage correspondent to the dehydration of the samples. In the Figures 1(a) and 1(c) is observed between 304-435 K and 305-418 K, a mass loss of approximately 9% and 7%, for energy cane and coconut fiber, respectively. According to Tabakaev et al. [14] and Jayaraman et al. [25], the mass loss in this stage occurs due to the moisture release and decomposition of light volatile compounds. In the heat flow (Q_{DSC}) curves, it is marked by an expressive endothermic peak (facing down) at 382 K (Figure 1b) and 352 K (Figure 1d), respectively, attributed mainly to water evaporation [20].

The second stage (435-745 K for energy cane, 418-677 K for coconut fiber) occurs the main biomass decomposition reactions, related to the breakdown of extractives, hemicellulose, cellulose, and partially of the lignin [9], [25]. For energy cane (Figures 1a and 1b), we observe in the evolution of the normalized mass (W), the greatest mass loss (56%). The normalized mass loss rate (dW/dt) and heat flow (Q_{DSC}) curves are marked by the presence of three peaks, referring to the extractives (499 K), hemicellulose (580 K), and cellulose (647 K) decompositions. For coconut fiber (Figures 1c and 1d), we verify a mass loss of 55%, and two peaks, associated with the hemicellulose (558 K) and cellulose (628 K) decompositions. In the normalized heat flow (Q_{DSC}) curves, for both biomasses, the two latter pseudocomponents are represented by exothermic reactions (facing up).

In the third stage (745-821 K for energy cane, 677-824 K for coconut fiber) occurs the carbonization of carbonaceous material [9], and no characteristic peak is observed in the normalized mass loss rate (dW/dt) curves (Figures 1a and 1c). In the normalized heat flow (Q_{DSC}) curves obtained for energy cane (Figure 1b) and coconut fiber (Figure 1d), it is noticed that the heat flow is not constant, however, neither endothermic nor exothermic behavior is observed. This was also observed in the He et al. [26] study.

In Table 2 it is presented the temperature ranges and the mass loss, the temperature peaks, and the maximum normalized mass loss rate $(dW/dt)_{max}$ and maximum heat flow $(Q_{DSC})_{max}$ correspondent at each stage of decomposition. The main differences occurred in the decompositions are due to the particularities of chemical composition (hemicellulose, cellulose, and lignin) of each biomass [13], [25].

Table 2. Temperature range and peaks of normalized mass loss rate, $(dW/dt)_{max}$, and normalized heat flow $(Q_{DSC})_{max}$ of three decomposition stages

Decomposition stage	Energy cane	Coconut fiber	
Dehydration			
Temperature range (K)	304-435	305-418	
Mass loss (%)	9	7	
$T_p(\mathbf{K})$	382	352	
dW/dt_{max} (1/s)	-3.9x10 ⁻⁴	-2.4x10 ⁻⁴	
Q_{max} (mW/mg)	-1.6	-1.3	
Volatilization			
Temperature range (K)	435-745	418-677	
Mass loss (%)	56	55	
$T_{p,E}\left(\mathbf{K}\right)$	499	-	
$dW/dt_{max,E}$ (1/s)	-5.1x10 ⁻⁴	-	
$Q_{max,E}$ (mW/mg)	-1.0	-	
$T_{p,HC}(\mathbf{K})$	580	558	
$dW/dt_{max,HC}$ (1/s)	-4.0x10 ⁻²	-1.2x10 ⁻³	
$Q_{max,HC}$ (mW/mg)	3.2	-0.19	
$T_{p,C}(K)$	647	628	
$dW/dt_{max,C}$ (1/s)	-4.5x10 ⁻²	-2.3x10 ⁻³	
$Q_{max,C}$ (mW/mg)	6.5	0.1	
Carbonization			
Temperature range (K)	745-821	677-824	
Mass loss (%)	9	8	
Final residue (%)	26	30	

Source: elaborated by the authors.

We emphasize that the present study had as a priority to evaluate the heat flow from the water contributions (Q_w) on heat flow from the experimental data (Q_{DSC}) and to define the specific heat capacity of biomasses $(c_{p,b})$ in the first stage of thermal decomposition (dehydration). Therefore, the subsequent analyses were carried out in the temperature ranges between 304 and 435 K and 305 and 418 K, for energy cane and coconut fiber, respectively.

3.2. Analysis of heat flow from water contributions

For the analyses of the water contributions on the heat flow from experimental data (Q_{DSC}) of both biomasses, it

was necessary to identify the point, in which the samples were water-free (Figure 1). This point is observed at the end of the first peak in the normalized mass loss rate (dW/dt=0), correspondent to the normalized mass (W_{wf}) of 0.9204 and 0.9512, in the temperature (T_{wf}) of 435 K and 418 K, for energy cane and coconut fiber, respectively. After defining these points, the normalized water mass was established, equation (6), at different times of the dehydration stage.

Thus, it was possible to determine the heat flow from the heat capacity of remaining water (Q_{wc}) and water evaporation (Q_{we}) , and the heat flow from the water contributions (Q_w) , as shown in Figures 2(a) and 2(b), for energy cane and coconut fiber, respectively. In these figures, the heat flow from the heat capacity of remaining water, Q_{wc} , are negligible compared to heat flow from the water evaporation, Q_{we} (phase change), which represent more than 90% of the heat flow from the water contributions (Qw) at temperatures above 356 K and 335 K, respectively. Similar behaviors were obtained by Artiaga et al. [19], Cai and Liu [20], and Chen et al. [27]. In these studies, the heat flow from the water evaporation (Q_{we}) represented more than 80% of the Q_{w} in the dehydration process.

3.3. Analysis of the specific heat capacity of biomasses (cp,b)

Figures 3(a) and 3(b) show the heat flow from experimental data (Q_{DSC}) , the heat flow from the water contributions (Q_w) , and heat flow from the heat capacity of biomass heating (Q_b) , for energy cane and coconut fiber, respectively.

375

(b)

400

425

450

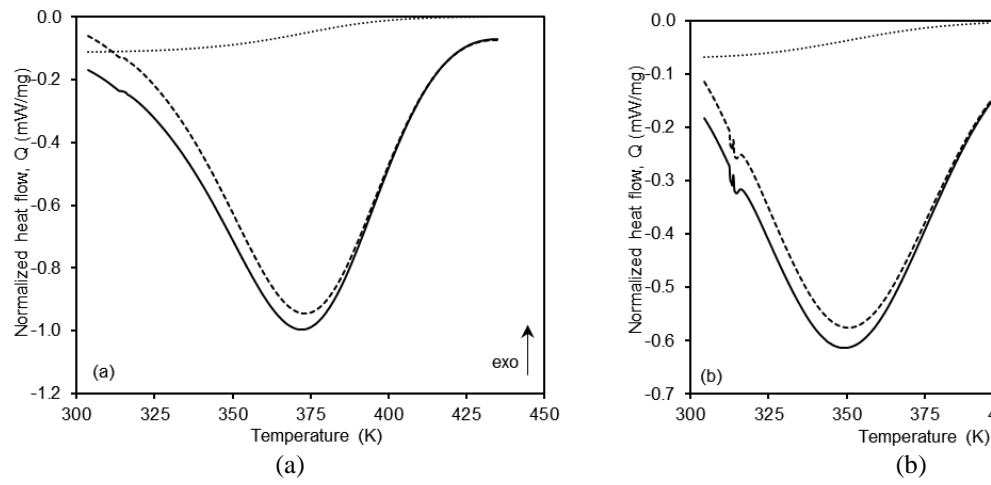


Figure 2. Normalized heat flow from the water contributions (Q_w) , heat capacity of remaining water (Q_{wc}) , and water evaporation (Q_{we}) as a function of temperature for energy cane (a) and coconut fiber (b). Source: elaborated by the authors.

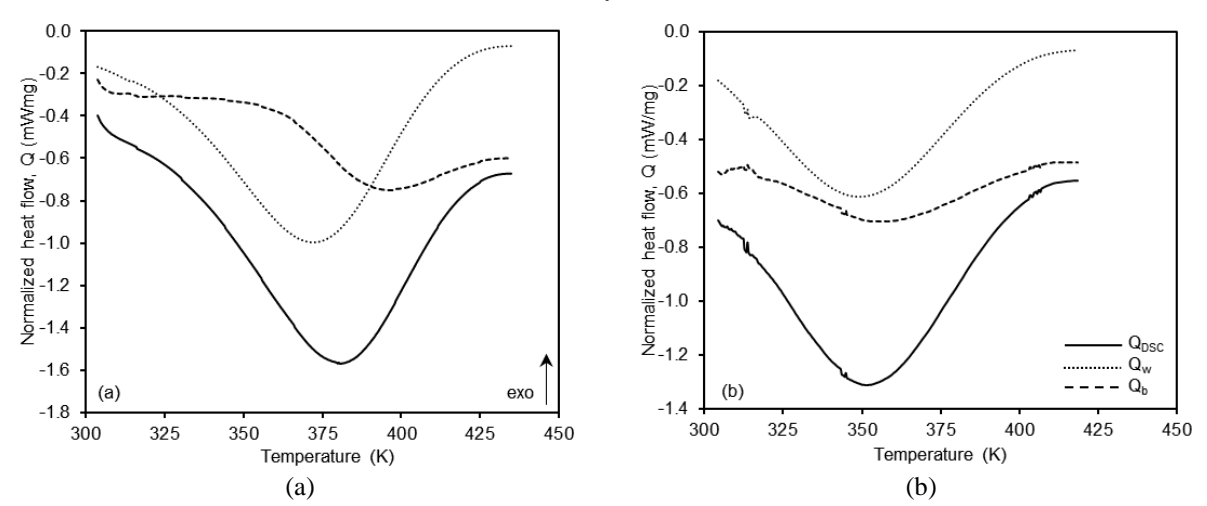


Figure 3. Normalized heat flow from the water contributions (Q_w) and heat capacity of biomasses (Q_b) as a function of temperature for energy cane (a) and coconut fiber (b). Source: elaborated by the authors.

Comparing heat flows from the heat capacity of biomasses (Q_b) in this figure, it is found significant influence by the different chemical compositions of biomass. The energy cane contains about 24% of extractives [9], not found in coconut fiber [22].

From the heat flow from heat capacity biomass heating (Q_b) in the dehydration stage, it was possible to determine the experimental specific heat capacity of them $(c_{p,b})_{exp}$ as a function of temperature (Figure 4). In this figure, the $(c_{p,b})_{exp}$, obtained by classical definition (equation 8) and ASTM E1269-11 (2018) (equation 9), show similar behaviors. Besides that, we verified that c_p curves present a peak at 386 K e 360 K, for energy cane and coconut fiber, respectively. This probably occurred due to the heat flow related to the release of low molecular weight compounds [25], above these peak temperatures. The representative peak was also observed in the study carried out by Wang et al. [28], in which three seaweeds were analyzed between 313 and 513 K, reaching a maximum at approximately 373 K.

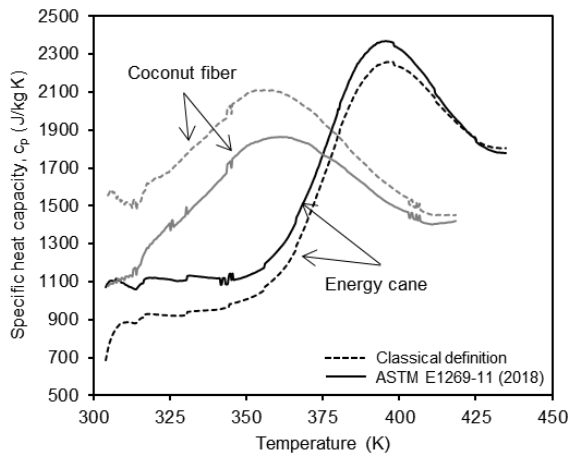


Figure 4. Experimental specific heat capacity $(c_{p,b})$ as a function of temperature for energy cane and coconut fiber. Source: elaborated by the authors.

Thus, for a better description of specific heat capacity for both biomasses during the dehydration stage, we

proposed theoretical polynomial equations, $(c_{p,b})_{theo}$, only for the specific temperature ranges (304-386 K and 305-360 K, respectively). These temperatures were established between initial temperature of the first stage and peak temperature characterized by the increasing of $(c_{p,b})_{exp}$ as shown in Figure 4.

The polynomial equations of $(c_{p,b})_{theo}$ (equations 11, 12, 13 and 14) and their respectives determination coefficients (R^2) are shown in Table 3 and illustrated in Figure 5(a). This property, determined by classical definition, ranged between 686-2260 J/kg K and 1452-2113 J/kg K, and through the ASTM E1269-11 (2018), between 1063 and 2371 J/kg K and 1076-1867 J/kg K, for energy cane and coconut fiber, respectively.

A few studies have been explored in the literature (Table 4) about the specific heat capacity, $c_{p,b}$, of biomasses. In the first study, Dupont et al. [2] applied the ASTM E1269-11 (equation 9) for obtaining this property in the temperature range of 313-353 K, disregarding the effect of the water contributions. In the second study, Comesaña et al. [21] applied the classical definition (equation 8), considering these contributions for the temperature range of 313-413 K. Part of these results, Figures 5(b) and 5(c), were compared in order to illustrate the variations achieved by different biomass and our experimental and theoretical data (Figure 5a).

We observed that for individual lignocellulosic compounds [21], Figure 5(b), the c_p varied from 1007 J/kg K to 2149 J/kg K for hemicellulose, from 1065 J/kg K to 2512 J/kg K for cellulose, and from 743 J/kg K to 2641 J/kg K for lignin (Figure 5b). For agricultural byproducts (brassica pellet, corn stover, olive pomace, olive stone, pinion, rice husk, wheat straw) and perennial crops (switchgrass) [2], [21], this property varied between 843 J/kg K and to 2680 J/kg K, shells (almond and hazelnut) [21], 923 J/kg K and 2585 J/kg K, and woods (oak, poplar, and pine pellets) [21], 705 J/kg K and 2808 J/kg K (Figure 5c).

Table 3. Proposal of polynomial equations for describing the theoretical specific heat capacity of biomasses

Method	Energy cane (304 K <t<386 k)<="" th=""><th>Coconut fiber (305 K<t<360 k)<="" th=""></t<360></th></t<386>	Coconut fiber (305 K <t<360 k)<="" th=""></t<360>
Classical definition	$c_p = -2.0 \times 10^{-4} \text{T}^4 + 0.2^2 \text{T}^3 - 1.2 \times 10^2 \text{T}^2 + 2.7 \times 10^4 \text{T} - 2.0 \times 10^6 $ $R^2 = 0.9942$ (11)	$c_p = -1.0 \times 10^{-2} \text{T}^3 + 10.0 \text{T}^2 - 3.3 \times 10^3 \text{T} + 3.7 \times 10^5$ (13) $R^2 = 0.9917$
ASTM E1269-11	$c_p = -1.0 \times 10^{-4} \text{T}^4 + 0.2 \text{T}^3 - 1.0 \times 10^2 \text{T}^2 + 2.5 \times 10^4 \text{T} - 2.0 \times 10^6 $ (12)	$c_p = -3.0 \times 10^{-3} \text{T}^3 + 3.7 \text{T}^2 - 1.1 \times 10^3 \text{T} + 1.3 \times 10^5 $ (14)
(2018)	$R^2 = 0.9904$	$R^2 = 0.9927$

Source: elaborated by the authors.

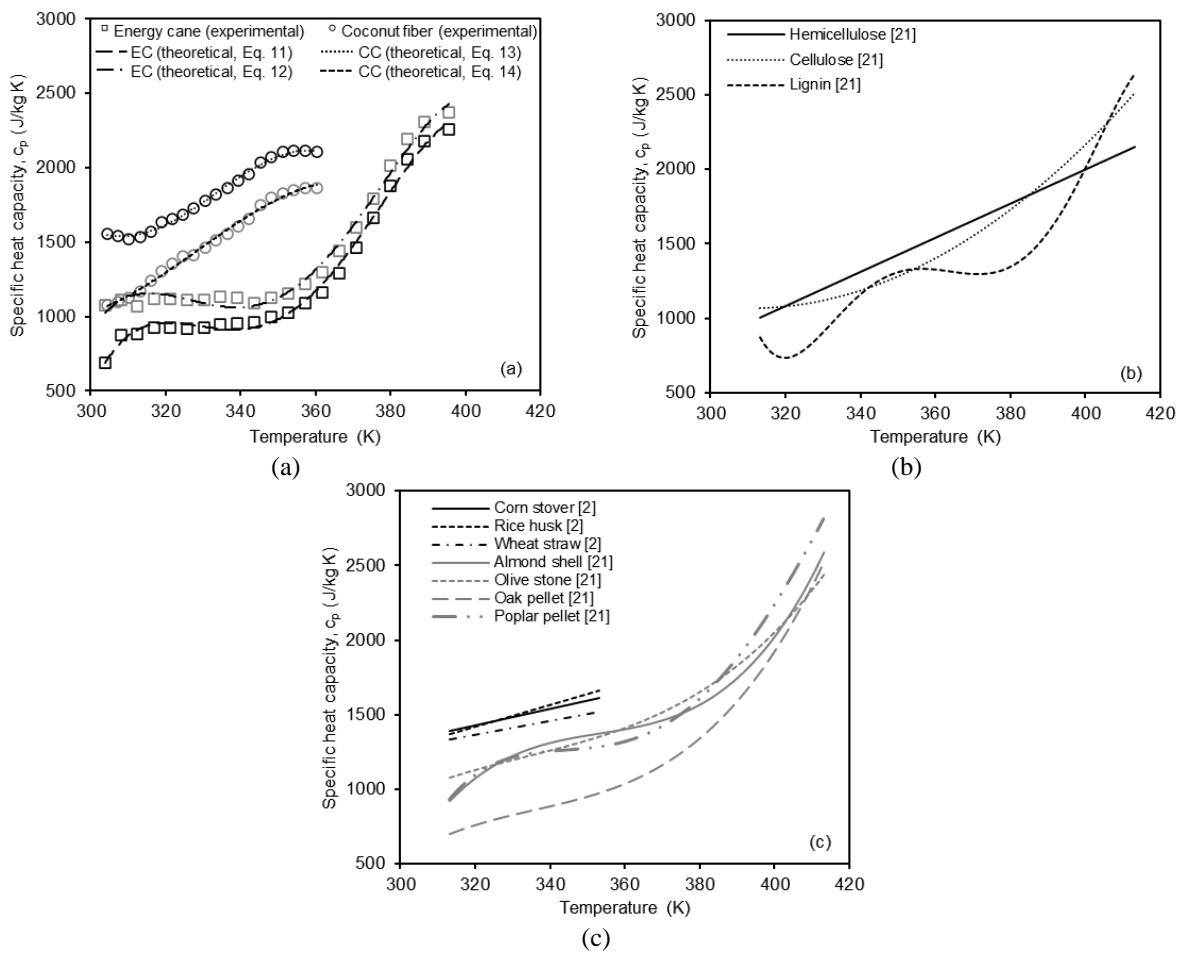


Figure 5. Specific heat capacity $(c_{p,b})$ profiles as a function of the temperature for energy cane and coconut fiber, and its respective polynomial equations (a); individual lignocellulosic compounds (b), and different kinds of biomasses from the literature (c). Source: elaborated by the authors.

Table 4. Polynomial equations of specific heat capacity for different biomasses from the literature

Reference	Material	Temperature range (K)	Specific heat capacity, $c_{p,b}$ (J/kg K)
Dupont et al. [2]	Corn stover	313-353	$c_p = 5.4\text{T}-284$
	Olive pomace		$c_p = 5.4\text{T}-333$
	Rice husk		$c_p = 7.2\text{T}-895$
	Switchgrass		$c_p = 4.9 \text{T} - 208 c_p$
	Wheat straw		$c_p = 4.8\text{T}-158$
Comesaña et al. [21]	Hemicellulose	313-413	$c_p = 11.4\text{T}-2.6\text{x}10^3$
	Cellulose		$c_p = 0.1T^2 - 85.2T + 1.4x10^4$
	Lignin		$c_p = -5.0 \times 10^{-6} \text{T}^5 + 9.7 \times 10^{-3} \text{T}^4 - 7.1 \text{T}^3 + 2.6 \times 10^3 \text{T}^2 - 4.7 \times 10^5 \text{T} + 3.0 \times 10^7$
	Almond shell		$c_p = 4.5 \times 10^{-3} \text{T}^3 - 4.8 \text{T}^2 + 1.7 \times 10^3 \text{T} - 2.0 \times 10^5$
	Hazelnut shell		$c_p = 3.7 \times 10^{-3} \text{T}^3 - 3.9 \text{T}^2 + 1.4 \times 10^3 \text{T} - 1.6 \times 10^5$
	Olive stone		$c_p = 1.4 \times 10^{-3} \text{T}^3 - 1.4 \text{T}^2 + 4.9 \times 10^2 \text{T} - 5.4 \times 10^4$
	Pinion		$c_p = 4.1 \times 10^{-3} \text{T}^3 - 4.4 \text{T}^2 + 1.5 \times 10^3 \text{T} - 1.8 \times 10^5$
	Brassica pellet		$c_p = 4.6 \times 10^{-3} \text{T}^3 - 4.9 \text{T}^2 + 1.7 \times 10^3 \text{T} - 2.0 \times 10^5$
	Oak pellet		$c_p = 2.6 \times 10^{-3} \text{T}^3 - 2.7 \text{T}^2 + 9.0 \times 10^2 \text{T} - 1.0 \times 10^5$
	Pine pellet		$c_p = 4.4 \times 10^{-3} \text{ T}^3 - 4.6 \text{ T}^2 + 1.6 \times 10^3 \text{ T} - 1.9 \times 10^5$
	Poplar pellet		$c_p = -5.0 \times 10^{-5} \text{T}^4 + 7.7 \times 10^{-2} \text{T}^3 - 43.9 \text{T}^2 + 1.1 \times 10^4 \text{T} - 1.0 \times 10^6$

Source: elaborated by the authors.

These specific heat capacities, $c_{p,b}$ are in the same magnitude order as those found in the present study (Figure 5a).

Furthermore, the equations (11)-(14) are in agreement with those suggested by Comesaña et al. [21] (Table 4). These authors obtained a linear equation for hemicellulose, second-order for cellulose and fifth-order temperature ranges analyzed. Regarding the $c_{p,b}$ of energy cane and coconut fiber, which presented polynomial equations of fourth- and third-order, respectively. The different trends of the equations occur due to the variability of the chemical composition of each biomass, in which can be more influenced by cellulose and lignin contents, as noted by Comesaña et al. [21].

4. Conclusions

The thermal decomposition of energy cane and coconut fiber was evaluated by simultaneous TG-DSC. The heat flow from experimental data (Q_{DSC}) presented an expressive endothermic peak corresponding mainly to the heat flow from water evaporation at the dehydration stage before the pyrolysis process. From the heat flow from heat capacity of each biomass (Q_b) , similar experimental profiles of specific heat capacity, $(c_{p,b})_{exp}$, were observed considering two methods, in which one peak was observed at 386 K and 360 K for energy cane and coconut fiber, respectively. The decrease in $(c_{p,b})_{exp}$, above these temperatures probably indicates the beginning of release of low molecular weight compounds by decreasing of this parameter. Thus, third- and fourthorder polynomial equations of $(c_{p,b})$ were proposed considering only the range between the initial and the peak temperatures. These equations showed good agreement with the experimental data and allow to estimate the energy required for biomass heating in the dehydration stage, as well as can be used in the pyrolytic reactor design.

5. Recommendations

Despite the good results and agreement with the literature, for future works, we recommend carrying out complementary analyses of the heat flow (Q_b) and specific heat capacity of biomasses $(c_{p,b})$, evaluating a possible effect of the remaining water in the samples. The samples should be heated from the initial temperature (298 K) until the beginning of decomposition (about 435 K for energy cane and 418 K for coconut fiber) and then restart the essays.

Funding

The authors thank the financial support received from the Coordination for the Improvement of Higher Education Personnel, CAPES (PROEX process number 0566/2017) and the National Council for Scientific and Technological Development, CNPq (Grant no. 142361/2016-0 and Grant no. 128184/2017-5), and for Espaço da Escrita/Pró-Reitoria de Pesquisa/UNICAMP for the language services provided.

Autor Contributions

F. Rezende-Lopes: Conceptualization, Investigation, Writing - Review & Editing, Writing - Review & Editing. K. Tannous: Conceptualization, Methodology, Writing - Review & Editing. T. Rezende-Lopes: Conceptualization, Investigation, Writing - Review & Editing.

All authors have read an agreed to the published version of the manuscript.

Conflicts of Interest

The authors declare no conflict of interest.

Institutional Review Board Statement

Not applicable.

Informed Consent Statement

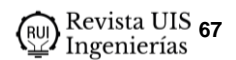
Not applicable.

References

[1] D.I. Aslan, B. Özoğul, S. Ceylan, F. Geyikçi, "Thermokinetic analysis and product characterization of Medium Density Fiberboard pyrolysis", *Bioresour. Technol.*, vol. 258, pp. 105-110, 2019, doi: https://doi.org/10.1016/j.biortech.2018.02.126

[2] C. Dupont, R. Chiriac, G. Gauthier, F. Toche, "Heat capacity measurements of various biomass types and pyrolysis residues", *Fuel*, vol. 115, pp. 644-651, 2014, doi: http://dx.doi.org/10.1016/j.fuel.2013.07.086

[3] Y.J. Rueda-Ordóñez, C.J. Arias-Hernández, J.F. Manrique-Pinto, P. Gauthier-Maradei, W.B. Bizzo, "Assessment of the thermal decomposition kinetics of empty fruit bunch, kernel shell and their blend", *Bioresour. Technol.*, vol. 292, pp. 121923, 2019, doi: https://doi.org/10.1016/j.biortech.2019.121923



- [4] F.X. Collard, J. Blin, "A review on pyrolysis of biomass constituents: Mechanisms and composition of the products obtained from the conversion of cellulose, hemicelluloses, and lignin", *Renew. Sustain. Energy Rev.*, vol. 38, pp. 594-608, 2014, doi: https://doi.org/10.1016/j.rser.2014.06.013
- [5] Y.J. Rueda-Ordóñez, K. Tannous, E. Olivares-Gómez, "An empirical model to obtain the kinetic parameters of lignocellulosic biomass pyrolysis in an independent parallel reactions scheme", *Fuel Process. Technol.*, vol. 140, pp. 222-230, 2015, doi: http://dx.doi.org/10.1016/j.fuproc.2015.09.001
- [6] Empresa de Pesquisa Energética- EPE. "Relatório Síntese -Ano base 2020", 2021. [Online]. Available at: https://www.epe.gov.br/sites-pt/publicacoes-dados-aber tos/publicacoes/PublicacoesArquivos/publicacao-601/t opico-588/BEN_S%C3% ADntese_2021_PT.pdf.
- [7] O.V. Carvalho-Netto, J.A. Bressiani, H.L. Soriano, C.S. Fiori, J.M. Santos, G.V.S. Barbosa, M.A. Xavier, M.G.A. Landell, G.A.G. Pereira, "The potential of the energy cane as the main biomass crop for the cellulosic industry", *Chem. Biol. Technol. Agric.*, vol. 1, pp. 1-8, 2014, doi: http://dx.doi.org/10.1186/s40538-014-0020-2
- [8] V.S. Carvalho, K. Tannous, "Thermal decomposition kinetics modeling of energy cane Saccharum robustum", *Thermochim. Acta*, vol. 657, pp. 56-65, 2017, doi: http://dx.doi.org/10.1016/j.tca.2017.09.016
- [9] H.R. Guimarães, K. Tannous, "Influence of torrefaction on the pyrolysis of energy cane: a study on thermal properties and decomposition kinetics", *J. Therm. Anal. Calorim.*, vol.139, pp. 2221-2233, 2019, doi: https://doi.org/10.1007/s10973-019-08584-z
- [10] Food and Agriculture Organization of the United Nation, FAOSTAT, 2021. [Online]. Available at: http://www.fao.org/faostat/en/#data/QC
- [11] A.S. Moura, R. Demori, R.M. Leão, C.L.C. Frankenberg, R.M.C. Santana, "The influence of the coconut fiber treated as reinforcement in PHB (polyhydroxybutyrate) composites", *Mater. Today Communi.*, vol. 18, pp. 191-198, 2019, doi: https://doi.org/10.1016/j.mtcomm.2018.12.006
- [12] J. Cai, S. Chen, "Determination of drying kinetics for biomass by thermogravimetric analysis under nonisothermal condition", *Dry. Technol.*, vol. 26, pp. 1464-1468, 2008, doi: https://doi.org/10.1080/0737390 802412116

- [13] D. Chen, D. Zhang, X. Zhu, "Heat/mass transfer characteristics and nonisothermal drying kinetics at the first stage of biomass pyrolysis", *J. Therm. Anal. Calorim.*, vol. 109, pp. 847-854, 2012, doi: https://doi.org/10.1007/s10973-011-1790-4
- [14] R.B. Tabakaev, A.V.Astafev, Y.V. Dubinin, N.A. Yazykov, A.S. Zavorin, V.A. Yakovlev, "Autothermal pyrolysis of biomass due to intrinsic thermal decomposition effects", *J. Therm. Anal. Calorim.*, vol. 134, pp. 1045-1057, 2018, doi: https://doi.org/10.1007/s10973-018-7562-7
- [15] A. Vega-Gálvez, M. Miranda, L.P. Díaz, L. López, K. Rodriguez, K. Di Scala, "Effective moisture diffusivity determination and mathematical modeling of the drying curves of the olive-waste cake", *Bioresour. Technol.*, vol. 101, pp. 7265-7270, 2010, doi: https://doi.org/10.1016/j.biortech.2010.04.040
- [16] D. Chen, Y. Zheng, X. Zhu, "In-depth investigation on the pyrolysis kinetics of raw biomass. Part I: Kinetic analysis for the drying and devolatilization stages", *Bioresour. Technol.*, vol. 131, pp. 40-46, 2013, doi: https://doi.org/10.1016/j.biortech.2012.12.136
- [17] Y.J. Rueda-Ordóñez, K. Tannous, "Drying and thermal decomposition kinetics of sugarcane straw by nonisothermal thermogravimetric análisis", *Bioresour. Technol.*, vol. 264, pp. 131-139, 2018, doi: https://doi.org/10.1016/j.biortech.2018.04.064
- [18] X. Li, C. Yin, "A drying model for thermally large biomass particle pyrolysis", *Energy Procedia*, vol. 158 pp. 1294-1302, 2019, doi: https://doi.org/10.1016/j.egypro.2019.01.322
- [19] R. Artiaga, S. Naya, A. García, F. Barbadillo, L. García, "Subtracting the water effect from DSC curves by using simultaneous TGA data", *Thermochim. Acta*, vol. 428, pp. 137-139, 2005, doi: https://doi.org/10.1016/j.tca.2004.11.016
- [20] J. Cai, R. Liu, "Research on Water Evaporation in the Process of Biomass Pyrolysis", *Energy & Fuels*, vol. 21, pp.3695-3697, 2007, doi: https://doi.org/10.1021/ef700442n
- [21] J.A. Comesaña, M. Nieströj, E. Granada, A. Szlek, "TG-DSC analysis of biomass heat capacity during pyrolysis process", *J. Energy Inst.*, vol. 86, pp. 153-159, 2013, doi: https://doi.org/10.1179/1743967112Z.00000 000055

- [22] F.C.R. Lopes, K. Tannous, "Coconut fiber pyrolysis decomposition kinetics applying single- and multi-step reaction models", *Thermochim. Acta*, vol. 691, pp. 178714, 2020, doi: https://doi.org/10.1016/j.tca.2020. 178714
- [23] F.C.R. Lopes, K. Tannous, "Coconut fiber pyrolysis: specific heat capacity and enthalpy of reaction through thermogravimetry and differential scanning calorimetry", *Thermochim. Acta*, vol. 707, pp. 179087, 2022, doi: https://doi.org/10.1016/j.tca.2021.179087
- [24] S. Vyazovkin, A.K. Burnhamb, J.M. Criado, L.A. Pérez-Maqueda, C. Popescu, N. Sbirrazzuoli, "ICTAC Kinetics Committee recommendations for performing kinetic computations on thermal analysis data", *Thermochim. Acta*, vol. 520, pp. 1-19, 2011, doi: https://doi.org/10.1016/j.tca.2011.03.034
- [25] K. Jayaraman, M.V. Kok, I. Gokalp. "Combustion properties and kinetics of different biomass samples using TG-MS technique", *J. Therm. Anal. Calorim.*, vol 127, pp. 1361-1370, 2017, doi: https://10.1007/s10973-016-6042-1
- [26] F. He, W. Yi, X. Bai, "Investigation on caloric requirement of biomass pyrolysis using TG–DSC analyzer", *Energy Convers. Manage.*, vol. 47, pp. 2461-2469, 2006, doi: https://doi.org/10.1016/j.enconman. 2005.11.011
- [27] D. Chen, M. Li, X. Zhu, "TG-DSC method applied to drying characteristics and heat requirement of cotton stalk during drying", *Heat Mass Transfer.*, vol. 48, pp. 2087-2094, 2012, doi: https://doi.org/10.1007/s00231-012-1050-6
- [28] S. Wang, X.M. Jiang, Q. Wang, H.S. Ji, L.F. Wu, J.F. Wang, S.N. Xu, "Research of specific heat capacities of three large seaweed biomass", *J. Therm. Anal. Calorim.*, vol. 115, pp. 2071-2077, 2014, doi: https://doi.org/10.1007/s10973-013-3141-0